Ab initio molecular-dynamics simulation of liquid As_xTe_{1-x} alloys

2009 J. Phys.: Condens. Matter 21 275602

(http://iopscience.iop.org/0953-8984/21/27/275602)

J. Phys.: Condens. Matter **21** (2009) 275602 (6pp) doi:10.1088/0953-8984/21/27/275602

Ab initio molecular-dynamics simulation of liquid As_xTe_{1-x} alloys

X F Zhu and L F Chen

Department of Physics, Nanjing Normal University, Nanjing 210097, People's Republic of China

Received 13 March 2009, in final form 20 May 2009
Published 10 June 2009
Online at stacks.iop.org/JPhysCM/21/275602

Abstract

Ab initio molecular-dynamics simulations have been used to investigate the structure and dynamics properties of the liquid alloy As_xTe_{1-x} at 800 K and at the five compositions $x = 0.2$, 0.3, 0.4, 0.5 and 0.6. We present results for the static structure factors, diffusion coefficients and frequency spectra, in addition to the electronic density of states. Both the results for the structural and dynamic properties are in relatively good agreement with the experimental data available. The results also indicate that the increase in the number of As atoms reduces the metallic character of the sample in close connection with a corresponding disruption of the Te chain structure.

(Some figures in this article are in colour only in the electronic version)

1. Introduction

Arsenic, tellurium and their alloys are good examples of systems in which the fine interplay of microscopic structure and electronic properties provides an interesting test ground for theories. The structure of liquid arsenic is found to be similar to its ground-state, rhombohedral crystal structure, with threefold coordination [1, 2]. A transformation should occur in liquid As from a threefold-coordinated semiconductor to a sixfold-coordinated metal when pressure is increased but not when temperature is increased [3]. The liquid metallic Te near the melting point has a covalently bonded chain structure composed of short and long bonds and the transition to the semiconducting state occurs in the supercooled liquid state [4, 5]. The measurements of the conductivity and Hall coefficient for liquid As–Te mixtures at different temperatures demonstrate that the liquid mixtures undergo a semiconductor to metal (S–M) transition above 500 °C and the transition temperature moves to higher temperature with increasing As concentration [6]. It was found that the network structure composed of threefold-coordinated As atoms and twofold-coordinated Te atoms is transformed into the chain structure near the S–M transition and that this 'network–chain' transformation is accompanied by volume contraction [7–10]. The metallic behavior observed for liquid As–Te mixtures at high temperature is primarily governed by the bonding configuration of Te atoms, and that the large fluctuations of the charge distribution in the shortened chains due to a frequent inter- and intrachain charge transfer induce the metallic conduction along the Te interchain direction [6]. However, *ab initio* molecular-dynamics simulations for liquid As_2Te_3 by Shimojo *et al* [11] show that the atomic structure does not transform into a chain-like structure but into some disordered structure and the electronic states around Te atoms contribute importantly to the metallization. Structural studies for liquid As–Te alloy have been extensively made by means of x-ray and neutron diffraction [7, 12–14], and extended x-ray absorption fine structure (EXAFS) techniques [6, 15, 16], and the structural information over a wider concentration has been determined for this liquid alloy. However, to our knowledge there is little theoretical work on the structural, dynamic and electronic properties of liquid As_xTe_{1-x} mixtures. It is obvious that an *ab initio* investigation of the properties of these systems might provide valuable information to clarify the experimental results. A detailed knowledge of the local environment around Te and As atoms and the electronic properties in the liquid mixture with different As concentrations allow a helpful understanding of the mechanism involved in the S–M transition. Therefore, in this paper we intend to explore the capabilities of the DFT approach in the generalized gradient approximation (GGA) to provide a realistic picture of various liquid As_xTe_{1-x} alloys ($x = 0.2$, 0.3, 0.4, 0.5, 0.6). We turn now to the body of this paper. In section 2, we briefly summarize our approach and method of calculation. Our results are presented extensively in section 3, together with some discussion. Finally, in section 4, we give a short conclusion.

Table 1. The densities of As_xTe_{1-x} at 800 K used in calculations. The experimental densities are taken from [8].

x	0.2	0.3	0.4	0.5	0.6
Density (g cm^{-3})	5.59	5.51	5.40	5.32	5.26

2. Computational methods

Our molecular-dynamics calculations have been performed by using the Vienna *ab initio* simulation program VASP [17, 18] with the projector augmented wave (PAW) method [19, 20]. The calculations presented here are based on density functional theory within the generalized gradient approximation (GGA). Our GGA calculations use the PW91 functional due to Perdew and Wang [21]. We have considered five concentrations of As_xTe_{1-x}: $x = 0.2$, 0.3, 0.4, 0.5 and 0.6. In each case, we used a cubic 100-atom supercell with periodic boundary conditions. For this size cell, the actual numbers of As atoms in the five samples were 20, 30, 40, 50 and 60. (Since the minority component in the 20% sample has only 20 atoms, the statistics will not be sufficient and the results should be given greatest significance for the majority component in this case.) The experimental densities used [8] at 800 K are shown in table 1. We use a 210 eV cutoff for the energies of the plane waves included in the wavefunction expansion and Γ-point sampling for the supercell Brillouin zone. For the electronic structure, we used Fermi-surface broadening corresponding to an electronic subsystem temperature of $k_BT = 0.1$ eV. In calculating the electronic wavefunctions, at each concentration we include ten empty bands. We control the ionic temperature using the Nosé–Hoover thermostat [22]. The equations of motion are integrated by means of the Verlet algorithm, using an ionic time step of 3 fs. The initial atomic configuration adopted was a random distribution of 100 atoms on the grid for each concentration. Then, the system is heated up to 2000 K by rescaling the ionic velocities. After equilibration for 4 ps at this temperature, we gradually reduce the temperature to 800 K. The physical quantities of interest were obtained by averaging over 10 ps after the initial equilibration taking 3 ps.

3. Results and discussion

3.1. Structural properties

The partial pair distribution functions obtained from the *ab initio* MD are depicted in figure 1. Our results for $g_{\alpha\beta}(r)$ at $x = 0.4$ are in close agreement with the recent calculation by Shimojo *et al* [11]. As shown in figure 1, the first-peak positions depend weakly on the x; $r_{\alpha\beta}$ is almost unchanged with increasing x since $r_{\alpha\beta}$ mainly corresponds to the bond length between α-and β-type atoms. Given the partial pair distribution functions, it is possible to calculate the average distances and partial coordination numbers as

$$\langle r\rangle = \frac{\int_0^{r_{\min}} r\,g_{\alpha\beta}(r)\,dr}{\int_0^{r_{\min}} g_{\alpha\beta}(r)\,dr}, \quad (1)$$

and

$$N_{\alpha\beta} = \int_0^{r_{\min}} 4\pi r^2 \rho_\beta g_{\alpha\beta}(r)\,dr, \quad (2)$$

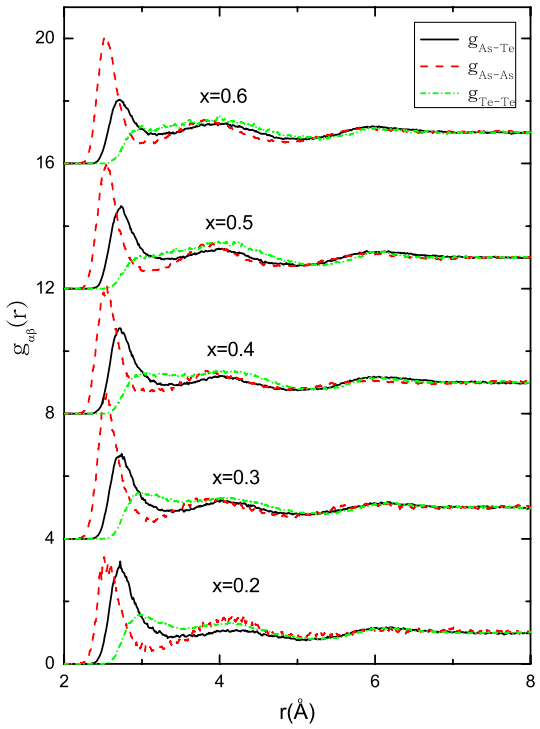

Figure 1. Atom–atom pair distribution functions $g_{AsAs}(r)$, $g_{TeTe}(r)$ and $g_{AsTe}(r)$ for l-As_xTe_{1-x} at a temperature of 800 K. The graphs are vertically offset by four units each for clarity.

where $r_{\min}$ is the position of the first minimum in the corresponding $g_{\alpha\beta}(r)$ and $N_{\alpha\beta}$ means the number of α atoms coordinated around the β atoms. The nearest-neighbor distances and the calculated partial coordination numbers of l-As_xSe_{1-x} are illustrated in table 2; the experimental data at 500 °C are also listed in table 2 for comparison. The As concentration dependence of $N_{\alpha\beta}$ is noticeable which is well in agreement with the experiments [6, 16]. The value of N_{TeTe} for $l - As_{0.2}Te_{0.8}$, which is very rich in Te content, is about 1 at 800 K while the EXAFS experiments on pure liquid Te [23] show that the chains in liquid Te with metallic properties are composed of short and long covalent bonds and the total coordination number is 1.8 at 500 °C. A large fraction of the bond in l-Te is considered to be broken upon the addition of As to liquid Te. There is a significant level of chemical disorder in l-As_xTe_{1-x} mixtures, marked by the existence of homopolar As–As and Te–Te pairs in the first coordination shell. The bonding energies reported in the literature [24] are 47.7 kcal mol^{-1} for As–As, 45 kcal mol^{-1} for As–Te and 38 kcal mol^{-1} for Te–Te bonds. The large difference in bonding energies between the As–Te and Te–Te bonds makes As atoms more likely to bind to Te atoms. The partial coordination number around Te, N_{TeTe}, reduces substantially upon the addition of As as seen in table 2; on the other hand, the coordination numbers around As atoms N_{AsTe} and N_{AsAs} approach 1.2 at $x = 0.5$. These results suggest that there appears in As-rich liquid mixtures a local atomic arrangement such as Te–As–As–Te where both ends of –As–As– are terminated by Te atoms. Thus it is considered that Te–Te bonds are less favored while As–As and As–Te are

Table 2. Nearest-neighbor distance r (in Å) and the calculated partial coordination number N for l-As_xTe_{1-x}. Experimental measurements at 500 °C are listed for comparison. The experimental data for $x = 0.3$ are taken from liquid $As_{33}Te_{67}$.

	As–As		As–Te		Te–As		Te–Te	
x	r	N	r	N	r	N	r	N
0.2	2.56	0.43	2.72	1.86	2.72	0.47	2.89	1.02
		0.48[a]		1.75[a]				
		0.48[b]		1.74[b]		0.41[b]		0.78[b]
0.3	2.55	0.87	2.72	1.54	2.74	0.66	2.89	0.82
		0.84[a]		1.43[a]				
		0.82[b]		1.40[b]		0.46[b]		0.67[b]
0.4	2.55	1.12	2.72	1.36	2.72	0.81	2.88	0.58
		0.93[a]		1.09[a]		0.82[a]		0.39[a]
	2.47[b]	0.96[b]	2.63[b]	1.06[b]	2.62[b]	0.80[b]	2.72[b]	0.37[b]
	2.50[c]	0.88[c]	2.68[c]	1.90[c]	2.68[c]	1.26[c]	2.85[c]	0.90[c]
0.5	2.54	1.29	2.73	1.19	2.73	1.19	2.89	0.44
0.6	2.54	1.65	2.72	0.79	2.72	1.20	2.89	0.40

[a] Reference [16]; [b] reference [6]; [c] reference [7].

more favored. The total coordination number of atom α in the alloy, N_α, can be obtained from the sum of partial coordination numbers, such as $N_{As} = N_{AsAs} + N_{AsTe}$. N_{As} in the liquid As–Te alloys stays to be about 2.4 in the whole composition range, implying that the covalent bonding and the corresponding local order in the solid phase (the As coordination number is about 3) is different from that of the liquid phase at 800 K. N_{Te} slightly increases with increasing As concentration, implying that it is more difficult in the liquid As–Te alloys to form a 'chain' structure in an As-rich concentration, which explains why the temperatures of the S–M transition move to higher temperature with increasing As concentration. We calculate the relative proportions of different As–Te(As) and Te–As(Te) coordinations, which vary from one-to fourfold. The coordination number is counted as the number of As(Te) atoms around As and Te atoms. The bond distances of As–As, As–Te and Te–Te are defined by the first minimum in the As–As, As–Te and Te–Te partial pair distribution functions. In figure 2, we just list two- and threefold-coordinated As and one-and twofold-coordinated Te, which are dominant with contributions. We can see that threefold-coordinated As and onefold-coordinated Te increase with increasing x; twofold-coordinated As decreases with increasing x and twofold-coordinated Te remains almost unchanged.

Since we are dealing with a mixture, an average $g(r)$ is obtained from the atom–atom distribution function $g_{\alpha\beta}(r)$ appropriately weighted with the atomic neutron scattering lengths:

$$g(r) = \frac{1}{\langle b\rangle^2}(x^2 b_{As}^2 g_{AsAs}(r) + (1-x)^2 b_{Te}^2 g_{TeTe}(r) + 2x(1-x)b_{As}b_{Te}g_{AsTe}(r)), \quad (3)$$

with $\langle b\rangle = x b_{As} + (1-x)b_{Te}$, x being the fraction of As atoms, and the scattering lengths $b_{As} = 0.658 \times 10^{-14}$ m and $b_{Te} = 0.58 \times 10^{-14}$ m. In order to make a proper comparison with neutron scattering data, the total structure factors $S(q)$, which are the Fourier transformation of the total pair distribution function, are shown in figure 3. The first peak of our calculated structure factors of l-As_xTe_{1-x} are in good agreement with experimental structure factors while the position of the second peak is a little larger than the experimental data. The observed $S(q)$ for $x = 0.2$ is similar to the $S(q)$ for liquid Te [25]. The first peak is higher than the second peak, which suggests that the interchain interaction plays an important role in the bonding configuration of this liquid mixture. The second peak of $S(q)$, which reflects the intrachain correlation, increases with increasing As concentration.

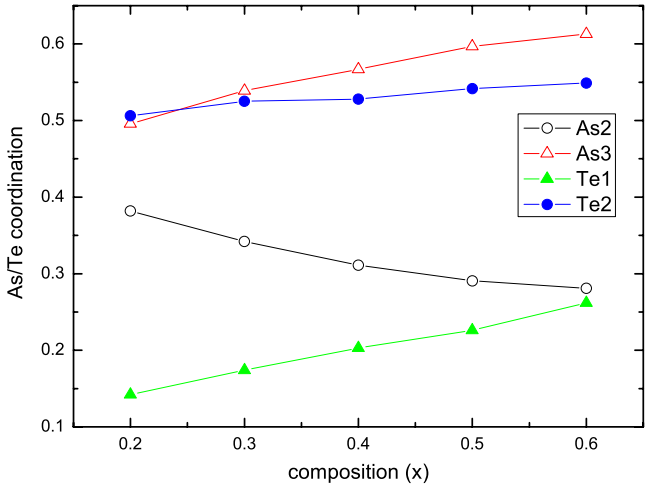

Figure 2. The coordination configurations of As and Te as a function of the composition x. Here the number besides As and Te indicates the coordination number. For example, As3 means the three-bonded As sites.

3.2. Dynamical properties

Focusing now on the dynamics, perhaps the most elementary property that can be evaluated from the MD runs is to derive the self-diffusion coefficient D from Einstein's relation, which correlates the time-dependent mean square displacement with the diffusion via

$$\langle [r(t) - r(0)]^2 \rangle \to 6Dt + \text{const}, \quad (4)$$

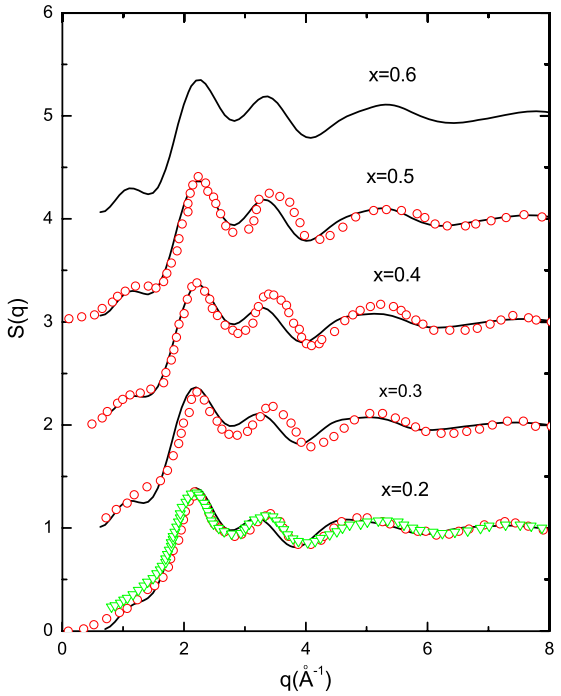

Figure 3. Calculated total structure factors for l-As_xTe_{1-x} (full lines) compared with the experimental results (circles [13], triangles [14]). The graphs are vertically offset by one unit each for clarity.

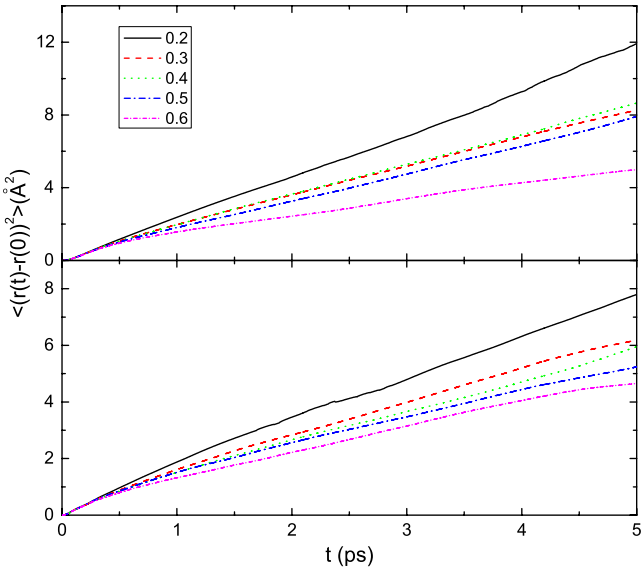

Figure 4. Mean square displacement of As (bottom panel) and Te (top panel) in l-As_xTe_{1-x} calculated by *ab initio* MD.

in the long time limit. The ensemble-averaged mean square displacement is plotted for each atomic species in figure 4 and we see that the diffusion rapidly reaches the linear regime. An alternative access to the diffusion coefficient is via the velocity autocorrelation function $C(t)$ defined by

$$C(t) = \frac{1}{3N}\left\langle \sum_{i=1}^{N} \frac{\mathbf{v}_i(t)\mathbf{v}_i(0)}{v_i(0)^2} \right\rangle. \tag{5}$$

The Fourier transform of $C(t)$ gives the frequency spectrum

$$Z(\omega) = \int_0^\infty C(t)\cos(\omega t)\,\mathrm{d}t. \tag{6}$$

The diffusion coefficient D is then given by

$$D = \frac{k_B T}{M} Z(0), \tag{7}$$

where k_B is Boltzmann's constant and M is the particle mass.

The self-diffusion coefficients calculated from the above two methods for the five compositions are given in table 3. Einstein's relation and the velocity autocorrelation function approaches for obtaining D suffer from the short timescales of our model and perhaps give an lower and upper bound on the actual value of D. The diffusion coefficients are of the same order of magnitude (10^{-9} m^2 s^{-1}) as for earlier calculated diffusion coefficients of liquid As [3] and Te [26]. The value for D_{Te} at $x = 0.2$ is a little larger than that obtained by a radioactive tracer method for pure l-Te ($D = 2.6 \times 10^{-9}$ m^2 s^{-1}) [27]. This difference is probably due to the lower temperature in the experiment. Te diffuses faster than As

Table 3. Diffusion constants (units of 10^{-9} m^2 s^{-1}) calculated from Einstein's relation (msd) and the velocity autocorrelation function (vacf).

	As		Te	
x	msd	vacf	msd	vacf
0.2	2.47(3)	2.39(2)	3.77(3)	3.94(6)
0.3	2.02(8)	2.34(7)	2.76(8)	3.31(7)
0.4	1.92(9)	2.12(4)	2.74(7)	3.07(5)
0.5	1.79(1)	1.90(5)	2.49(6)	2.51(4)
0.6	1.64(1)	1.77(6)	1.89(8)	1.93(9)

and the diffusion of both species decreases with As content. Notice that As–As and As–Te bonds are stronger than Te–Te bonds and that the presence of As increases the As–As and As–Te bonds, it is understandable that diffusion constants decrease in parallel with the ratio of As in the sample, and that As atoms should have more difficulties to diffuse than Te atoms.

The Fourier transform gives the frequency spectrum, which will give us, among other things, information on the vibrational modes of the sample. In figure 5 we have collected the frequency spectra for the five systems under consideration. The most relevant feature worth mentioning is the shift in the low-frequency torsion band towards higher energies as the number of As atoms increases. This relative shift of frequency spectra is due to the change of the dominant building blocks. The effective valence force field undergoes a global change with the increasing As concentration. A high-energy bond stretching band appears and the peak is enhanced as the number of As atoms increases. This is clearly due to the bonds in which As atoms are involved, since in the spectrum of pure Te no excitations are present for energies greater than 20 meV [28]. A shift toward higher energies is also observed in the bond stretching band which is due to the strengthening of the bonds as As atoms are incorporated into the structure.

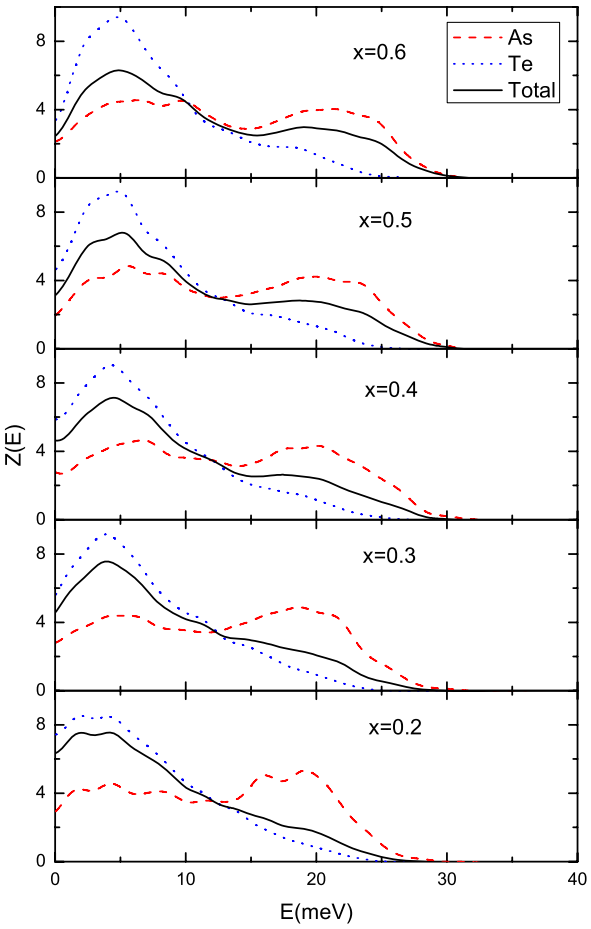

Figure 5. Frequency spectra for l-As_xTe_{1-x} alloys calculated by *ab initio* MD.

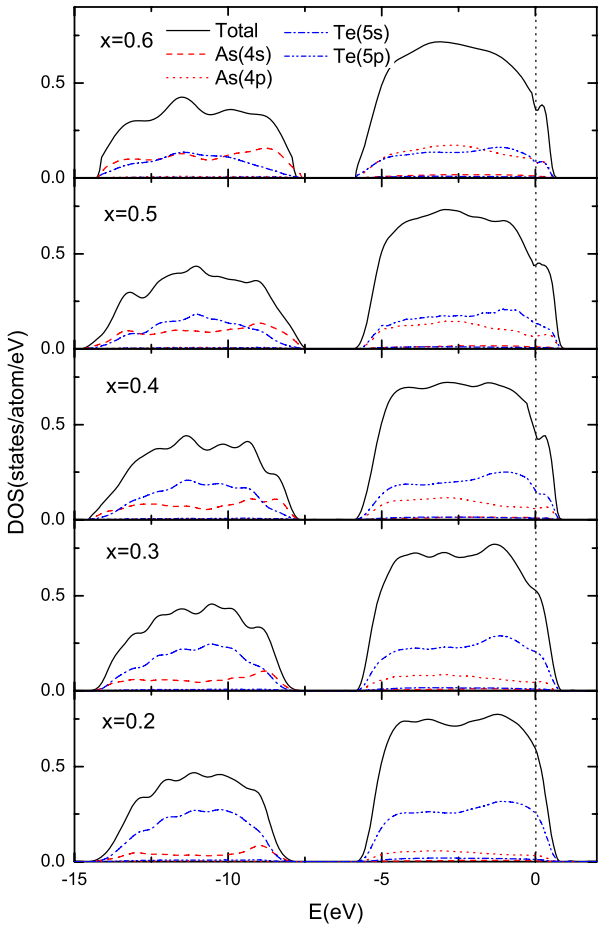

Figure 6. The electronic density of states for l-As_xTe_{1-x} alloys calculated by *ab initio* MD. The energy zero is taken at the Fermi level (vertical dotted line).

3.3. Electronic structure

The structural behavior of liquid alloys can also be understood in terms of the electronic structure. In figure 6 we have plotted the change in the electronic density of states (DOS) as the As concentration increases. The lowest band between about -14 and -8 eV originates from the atomic s-like states of As and Te which is essentially identical for all the concentrations. The next band above -6 eV contains p-like states of As and Te. The liquid mixture has metallic properties in Te-rich concentration. Actually, for the temperature under consideration, the electrical conductivity of pure liquid Te has reached a value of $2.4 \times 10^5\ \Omega^{-1}\ \mathrm{m}^{-1}$ [29]. A dip appears at the Fermi level when $x \geqslant 0.4$ which means that the metallic character decreases with increasing As concentration. The identification of these features is made straightforward by the examination of the partial DOS of the As and Te atoms, which are also displayed in figure 6. This metal–semiconductor properties transition is closely related to the electronic structure around the Te atoms. In Te two of the four p electrons form the σ-bonds between neighboring atoms and the retained two electrons occupy the lone pair (LP) orbital. The metallic properties of l-Te arise from a frequent charge transfer from LP orbitals to antibonding orbitals in the neighboring chains by thermal agitation. A substantial decrease of N_{TeTe} is observed upon the addition of As as shown in table 2. This implies that Te–Te bonds substantially reduce upon the addition of As owing to the significant difference in the bonding energies between As–Te and Te–Te bonds. Te atoms in the chain are replaced by As atoms upon the addition of As to liquid Te. As atoms play a role in binding the neighboring chains to stabilize the network structure with threefold-coordinated As sites which restrains large fluctuations of the charge distribution in the chains.

4. Conclusions

The As concentration dependence of structural, dynamics properties and electronic properties in the liquid As–Te mixture at 800 K has been investigated by means of *ab initio* MD simulations. The structural analysis of $g(r)$ for $x = 0.2$ gives the most reliable information on the partial correlation of Te, since the contribution of the pair correlation of As–As is negligible. The total coordination number for the Te, N_{Te}, slightly increases with increasing As concentration, implying that it is more difficult in the liquid As–Te alloys to form 'chain' structures in As-rich concentration. The As atoms play a role in binding the neighboring chains to stabilize the network structure with threefold-coordinated As sites which may enhance the S–M transition temperature in liquid As–Te

alloys. The electronic structure calculations also show that the metallic character of As–Te alloys decreases with increasing As concentration.

Acknowledgment

Numerical calculations were carried out using the facilities of the Department of Physics in Nanjing Normal University.

References

[1] Bellissent R, Bergman C, Ceolin R and Gaspard J P 1987 *Phys. Rev. Lett.* **59** 661
[2] Hafner J 1989 *Phys. Rev. Lett.* **62** 784
[3] Li X P 1990 *Phys. Rev.* B **41** 8392
[4] Tsuzuki T, Yao M and Endo H 1995 *J. Phys.: Soc. Japan* **64** 485
[5] Tsuchiya Y 1991 *J. Phys.: Condens. Matter* **3** 3163
[6] Endo H, Hoshino H, Ikemoto H and Miyanaga T 2000 *J. Phys.: Condens. Matter* **12** 6077
[7] Kameda Y, Usuki T and Uemura O 1996 *J. Non-Cryst. Solids* **205–207** 130
[8] Tsuchiya Y 1999 *J. Non-Cryst. Solids* **250–252** 473
[9] Oberafo A A 1975 *J. Phys. C: Solid State Phys.* **8** 469
[10] Hoshino H, Miyanaga T, Ikemoto H, Hosokawa S and Endo H 1996 *J. Non-Cryst. Solids* **205–207** 43
[11] Shimojo F, Hoshino K and Zempo Y 2002 *J. Phys.: Condens. Matter* **14** 8425
[12] Ma Q, Raoux D and Benazeth S 1996 *J. Non-Cryst. Solids* **205–207** 130
[13] Usuki T, Itoh K, Kameda Y and Uemura O 1998 *Mater. Trans. JIM* **39** 1135–9
[14] Maruyama K, Hoshino H, Ikemoto H, Miyanaga T and Endo H 2002 *J. Non-Cryst. Solids* **312–314** 356
[15] Tamura K, Hosokawa S, Inui M, Yao M and Endo H 1993 *J. Non-Cryst. Solids* **156–158** 712
[16] Ikemoto H, Hoshino H, Miyanaga T, Yamamoto I and Endo H 1999 *J. Non-Cryst. Solids* **250–252** 458
[17] Kresse G and Furthmuller J 1996 *Comput. Mater. Sci.* **6** 15
[18] Kresse G and Furthmuller J 1996 *Phys. Rev.* B **54** 11169
[19] Blöchl P E 1994 *Phys. Rev.* B **50** 17953
[20] Kresse G and Joubert D 1999 *Phys. Rev.* B **59** 1758
[21] Wang Y and Perdew J P 1991 *Phys. Rev.* B **44** 13298
[22] Nosé S 1984 *J. Chem. Phys.* **81** 511
Hoover W G 1985 *Phys. Rev.* A **31** 1695
[23] Kawakita Y, Yao M and Endo H 1999 *J. Non-Cryst. Solids* **250–252** 447
[24] Nandakumar K and Philip J 1992 *J. Non-Cryst. Solids* **142** 247
[25] Misawa M 1992 *J. Phys.: Condens. Matter* **4** 9491
[26] Lomba E, Katcho N A and Otero-Díaz L C 2005 *Phys. Rev.* B **72** 134201
[27] Kurlat D H, Potard C and Hicter P 1974 *Phys. Chem. Liq.* **4** 183
[28] Endo H, Tsuzuki T, Yao M, Kawakita Y, Shibata K, Kamiyama T, Misawa M and Suzuki K 1994 *J. Phys. Soc. Japan* **63** 3200
[29] Li C, Su C-H, Lehoczky S L, Scripa R N, Lin B and Ban H 2005 *J. Appl. Phys.* **97** 083513